

Design of a 4.9 to 6.0 GHz Two-stage Low Noise Amplifier for 802.11a, HiperLAN2 and HiSWANa Receivers Using ATF-551M4 E-PHEMT

Application Note 5091

This application note examines the design of a compact (6 mm by 15 mm) two-stage, low noise, unconditionally stable, amplifier for 802.11a, HiperLAN2 and HiSWANa receiver applications. At 5.5 GHz and biased at 3.3 V and 30 mA, the amplifier provides 22.2 dB gain, 1.4 dB noise figure, linear output power (P_{1dB}) of +11.5 dBm, and a third-order output intercept point (OIP3) of +28 dBm. Its frequency coverage includes the portions of the 5 GHz spectrum currently specified for wireless local-area networking in North America, Europe and Japan:

North American 802.11a:

5.15-5.35 GHz and 5.725-5.825 GHz
(U-NII bands)

European HiperLAN2:

5.15 - 5.35 and 5.470 - 5.725 GHz,

Japanese HiSWANa:

5.15-5.25 GHz

The amplifier is designed around the Agilent ATF-551M4 low noise enhancement mode pseudomorphic HEMT (EpHEMT) in both stages. The device is supplied in a leadless surface-mount plastic package with dimensions of 1.4 mm x 1.2 mm x 0.7 mm, and its 400- μ m gate width combines low noise figure coincident with high intercept point over the 2 to 10 GHz frequency range.

Besides having a very low typical noise figure (0.5 dB), the ATF-551M4 is specified at 2 GHz and 2.7-volt bias to provide a +24.1 dBm thirdorder output intercept point (OIP3) at 10 mA drain current.

The advantage of an enhancement mode PHEMT versus a depletion mode PHEMT is that biasing the device is simplified by the fact that the enhancement mode PHEMT requires a positive voltage on the gate for normal biasing as opposed to a negative voltage for a depletion mode PHEMT. Biasing the ATF-551M4 only requires a voltage divider from the drain to supply a small positive voltage to the gate for nominal drain current.

A data sheet for the ATF-551M4 may be downloaded from:
(<http://cp.literature.agilent.com/lit-web/pdf/5988-9006EN.pdf>)

Low noise E-pHEMT amplifier design

To meet the goals for noise figure and gain, the drain source current (I_{DS}) of each stage was chosen to be 15 mA. According to the data sheet this value provides good IP3 combined with a very low minimum noise figure (F_{min}). The data sheet also indicates that a 2.7 V drain-to-source voltage (V_{DS}) gives slightly higher gain and easily allows the use of a regulated 3.3 V supply.



Agilent Technologies

Using Agilent Technologies EEs of Advanced Design System software (ADS) the amplifier circuit can be simulated in both linear and non-linear modes of operation. For the linear analysis the transistors can be modeled with a two-port sparameter file using Touchstone format. File ATF551M4.s2p can be downloaded from the Agilent Wireless Design Center web site (<http://www.agilent.com/view/rf>). In addition to information regarding gain, noise figure, and input and output return loss, the simulation also provides important insight into circuit stability. Calculating the Rollett stability factor (K) and generating stability circles are both made considerably easier with computer simulation.

The ADS nominal optimization (also known as performance optimization) tool was used to aid the amplifier design. This tool can be used to modify a set of parameter values to satisfy predetermined performance goals by comparing computed and desired responses and modifying design parameter values to bring the computed response closer to target performance. Nominal optimization

is available in the ADS simulator for analog/RF systems simulation using any analysis type, such as AC, DC, S-parameter, harmonic balance, circuit envelope, and transient simulation. Goals were set for gain, noise figure and return loss over the 4.9 - 6.0 GHz bandwidth, out-of-band gain, as well as for unconditional stability from 0.1 – 18 GHz. An example of nominal optimization, optex1_prj, is available in Chapter 2 of the ADS help library under *tuning, optimization and statistical design*.

For the optimization tool to work at 6 GHz, accurate equivalent circuit models for the resistors, inductors and capacitors are required. The models must include package parasitic inductance, resistance and capacitance, which allows the component value to be varied over a small range using the optimization tool and accurately correlate to measured data. Examples of passive component models and ADS optimization tool terminology are shown in Fig.1. It should be noted that each manufacturer's passive elements exhibit slightly different parasitic properties.

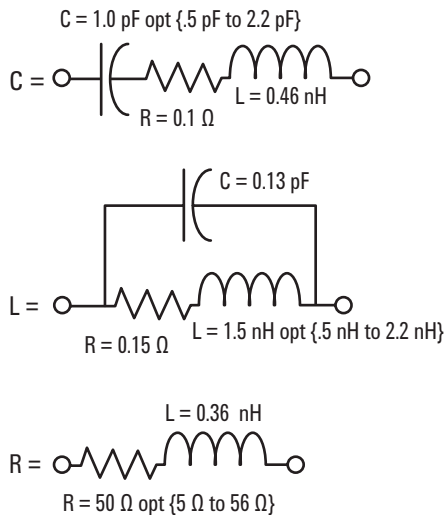


Figure 1. Passive component models and ADS optimization tool terminology

The demonstration board shown in Fig. 2 was developed primarily for 5 to 6 GHz applications. The demonstration board is a two layer configuration for rigidity. The printed circuit board material is FR-4 with a typical dielectric constant of 4.2 and a total board thickness of 0.052 inches. The signal layer is the top layer which is 0.010 inch thick while the bottom layer is 0.042 inch thick. The RF input and output connectors, J1 and J2, are normally designed for 0.062 inch thick printed circuit boards. The center pin is trimmed to about 0.040 inches in length and then the connectors are installed such that the center pin lays down directly on the printed circuit board with no gap between the printed circuit board and center pin. Be sure to solder both the top and bottom ground pins of the connectors to the printed circuit board.

The board utilizes small EIA 0402 (.04 x .02 in/ 1.0 x 1.5 mm, nominal) form-factor

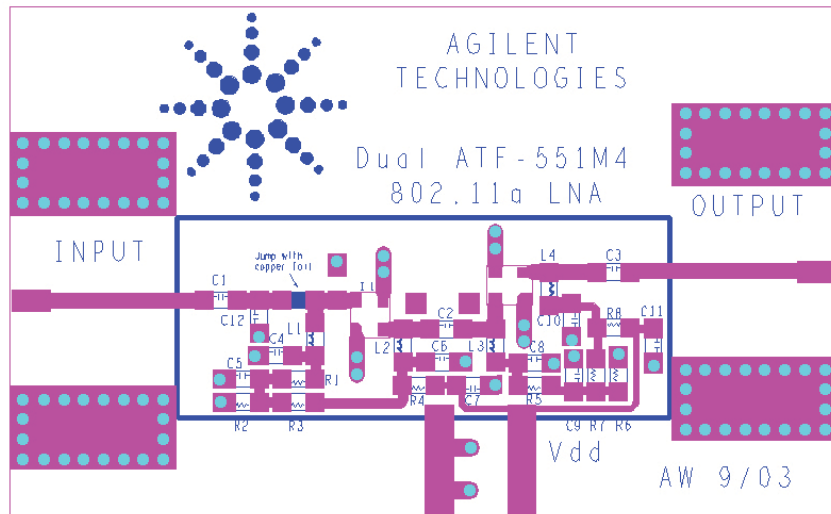


Figure 2. Demonstration Board Artwork and Component Placement

surface mount components. The use of microstrip lines in place of the 0402 inductors would reduce circuit losses but would produce a larger layout. The actual 6 mm by 15 mm area required for the circuitry is outlined in blue.

The schematic diagram of the two-stage amplifier is shown in Fig. 3. The amplifier uses a bandpass network for input matching and a high-pass network for output matching. Interstage matching is provided by a high pass network. The parts list is shown in Table I.

The input network represents a compromise between best noise figure and reasonable input return loss and consists of series capacitor C1, shunt inductor L1 and shunt capacitor C12. Note that when using the demonstration board layout shown, the mounting pads before L1 will have to be bridged with copper foil. The mounting pads are included to allow for a low-pass impedance matching network topology if desired for individual application requirements.

The output high-pass network consists of a series capacitor C3 and a shunt inductor L4. The bandpass and high-pass networks provide additional low frequency gain roll-off which serves several purposes.

Table 1. Component parts list for 2 stage ATF-551M4 amplifier

C1, C4	2.2 pF Johnson 251R07C2R2BV4E
C2	0.8 pF Johnson 251R07C0R8BV4E
C3	3.9 pF Johnson 251R07C3R9BV4E
C5, C7, C9, C11	10 nF Kemet C0402C103K3RACTU
C6	1.0 pF Johnson 251R07C1R0BV4E
C8, C10	1.5 pF Johnson 251R07C1R5BV4E
C12	0.5 pF Johnson 251R07COR5BV4E
L1, L2, L3, L4	1.5 nH Johnson L-07C1N5S
J1, J2	E.F. Johnson SMA connector 142-0701-801
R1, R5	49.9 Ω Yageo 9C04021A49R9FLHF3
R2, R6	5.1K Ω Yageo 9C04021A5101JLHF3
R3, R7	22K Ω Panasonic ERJ-2RKF222X
R4, R8	39 Ω Yageo 9C04021A39R0FLHF3
Q1, Q2	Agilent ATF-551M4

First, enhanced rejection of lower frequency signals may decrease the susceptibility of the LNA to stronger low frequency emitters, which could drive the LNA to compression and adversely affect the in-band performance. Second, the roll-off of the low frequency gain also improves the stability of the LNA, since a low frequency gain peak is generally associated with a decreased value of K. Since L1 is also used for the insertion of gate voltage, the inductance must be adequately bypassed at the normal operating frequency by C4. Resistor R1 and C5 provide a good low frequency resistive termination, which

enhances low frequency stability. If the value of C4 is made too large, the series-resonant frequency of L1 and C4 can often produce a low frequency gain resonance, which may prove difficult to stabilize with R1 and C5. With the help of the optimization function in ADS, values for L1, C4, and R1 can be selected for best low frequency stability. C5 is 10 nF to improve the output third-order intercept and is kept constant during the optimization process. In a similar fashion, L4 is used to apply drain voltage to Q2 and is therefore bypassed with C10. R8 and C11 provide a low frequency resistive termination.

Since the primary goal of the input network is to provide a low noise figure coincident with good S11 and the primary goal of the output network is to provide the desired power output with good S22, the interstage network can be called upon to help flatten gain over the desired bandwidth, to decrease gain at lower frequencies and to help with overall stability. With inductors required to apply drain voltage to Q1 and gate voltage to Q2, and a capacitor required for DC isolation between the two stages, we have the basis for a high pass network. ADS is used to optimize this network for the various parameters. In a similar fashion, R4/C7 and R5/C9 provide low frequency bias decoupling and enhance low frequency stability.

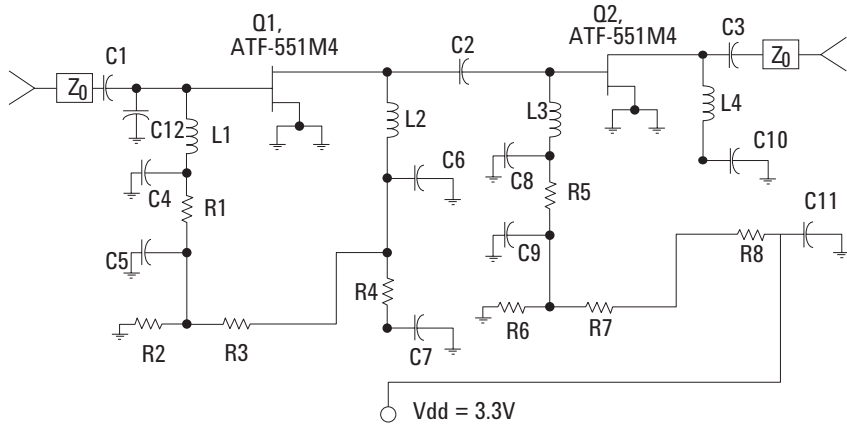


Figure 3. Schematic Circuit Using Passive Bias

to Q1 and gate voltage to Q2, and a capacitor required for DC isolation between the two stages, we have the basis for a high pass network. ADS is used to optimize this network for the various parameters. In a similar fashion, R4/C7 and R5/C9 provide low frequency bias decoupling and enhance low frequency stability.

Source Grounding

The importance of properly grounding the source terminals of the FETs cannot be overemphasized. Quite often, the designer feels that the only proper way to ground the sources is with the shortest distance possible between the device and the signal ground plane. Although the shortest length will generally provide the highest gain, some controlled amount of source inductance can be used to increase stability, improve S11 and S22 with minimal effect on noise figure and only a slight reduction in gain. In some cases where the distance between the source terminals and the ground plane is excessive, the amplifier will have uncontrollable oscillations that are most likely up in the 8 GHz and higher frequency range.

This amplifier design makes use of a small amount of source inductance in the form of a short length of microstrip between each source terminal and the plated through hole that connects the top layer etch to the signal ground plane. With any multi-layer circuit board, it is very important that the plated through holes for any top layer circuitry make contact with the ground plane directly beneath the signal layer. The plated through holes can continue on to the lower layers but must not skip over the very important signal ground plane. Unnecessarily long grounds can cause undesired feedback and result in amplifier instabilities and oscillations.

Accurately modeling the microstrip line dimensions between each source terminal and the plated through hole and the plated through hole dimensions between the microstrip and the signal ground plane will allow the designer to use ADS to determine the optimum amount of source inductance for a given design. Since source inductance generally makes the FETs regenerative at higher frequencies and degenerative at lower frequencies, a plot of K from 100 MHz to 18 GHz will reveal an optimum amount to be used in the circuit.

Biasing

Once the RF matching has been established, the next step is to DC bias the device. A passive biasing example is shown in Fig. 3. In this example the voltage drop across resistor R4 and R8 sets the drain current (I_d), with their values calculated using the following equation:

$$R_4 = R_8 = \frac{V_{dd} - V_{ds}}{I_{ds} + I_{bb}}$$

Equation 1.

where:

V_{dd} is the power supply voltage, 3.3 V;

V_{ds} is the device drain to source voltage, 2.7 V;

V_g is the device gate to source voltage, 0.515 V;

I_{ds} is the device drain to source current, 15 mA;

I_{bb} for DC stability is 10 times the typical gate current, 0.1 mA.

Voltage divider networks R2/R3 and R6/R7 establish the typical gate bias voltage (V_g).

$$R_2 = R_6 = \frac{V_g}{I_{bb}}$$

Equation 2.

$$R_3 = R_7 = \frac{(V_{ds} - V_g) \times R_2}{V_g}$$

Equation 3.

The complete passive bias example may be found on page 20 of the product data sheet (<http://literature.agilent.com/litweb/pdf/5988-9006EN.pdf>). Note that there are differences between calculated values and the actual values due to the use of preferred component values as shown in Table 1.

As with any depletion or enhancement mode PHEMT, the dc parameter variation from device to device can cause the quiescent drain current to either increase or decrease from the nominal design value. Active biasing provides a means of keeping the quiescent bias point constant as dc parameters may vary from lot to lot. Active biasing also provides bias stability over temperature and is the recommended method of biasing any PHEMT device in high volume applications.

Results

The amplifier is tested at a power supply voltage V_{dd} of 3.3 V, which provides each device with a bias point of $V_{ds} = 2.7$ V @ $I_d = 15$ mA. The measured performance is compared to the simulated performance which is obtained from the device data sheet S and noise parameters. The measured and simulated noise figure is shown in Fig. 4. Noise figure is a nominal 1.4 dB at 5.8 GHz. The loss of the input microstripline has been measured at 0.15 dB, making the noise figure of the device plus the loss of the matching network around 1.25 dB. The output power at 1 dB gain compression, $P_{1\text{dB}}$, was measured as +11.5 dBm. The output third-order intercept point, OIP3, was measured at +28 dBm.

The measured and simulated gain of the amplifier is a nominal 22 dB at 5.8 GHz. The swept gain plot shown in Fig. 5 shows moderate gain roll-off at lower frequencies. Measured and simulated input and output return loss is shown in Figure 6 and 7, respectively. The measured input return loss is greater than 10 dB over the 4.9 to 6 GHz frequency range while the output return loss measured greater than 9.5 dB over the same frequency range.

Table 2 provides a summary of the performance of the amplifier over the expected battery operating conditions. It was noted that at 3.6V, a fully charged battery, the noise figure performance was unaffected. The table also shows that as the battery voltage drops below 3V, only a small degradation in performance is observed.

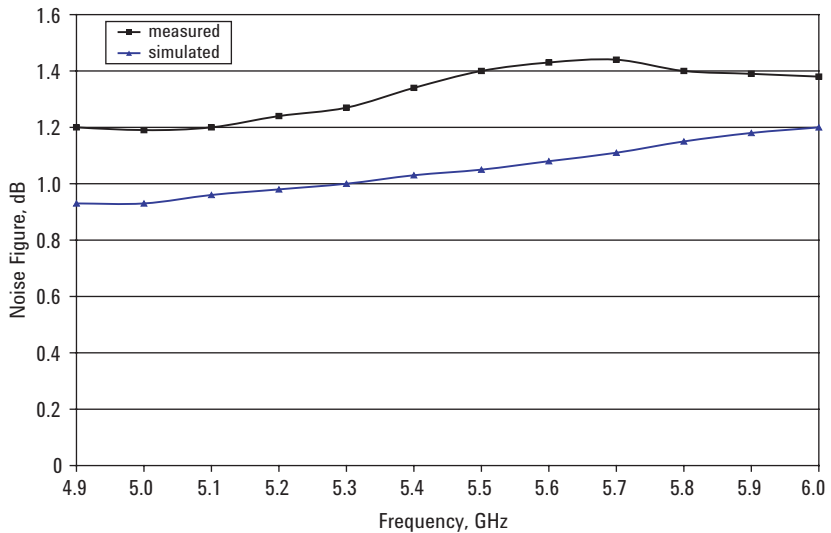


Figure 4. Measured and Simulated Noise Figure vs. Frequency

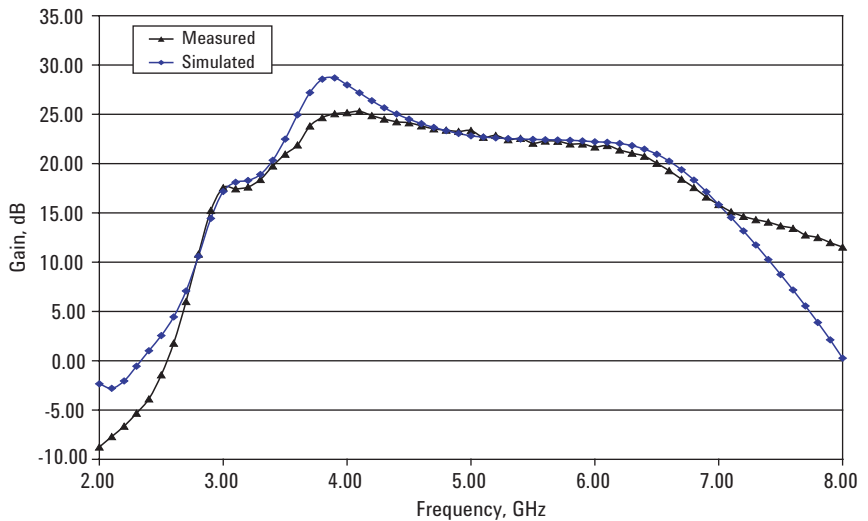


Figure 5. Measured and Simulated Gain vs. Frequency

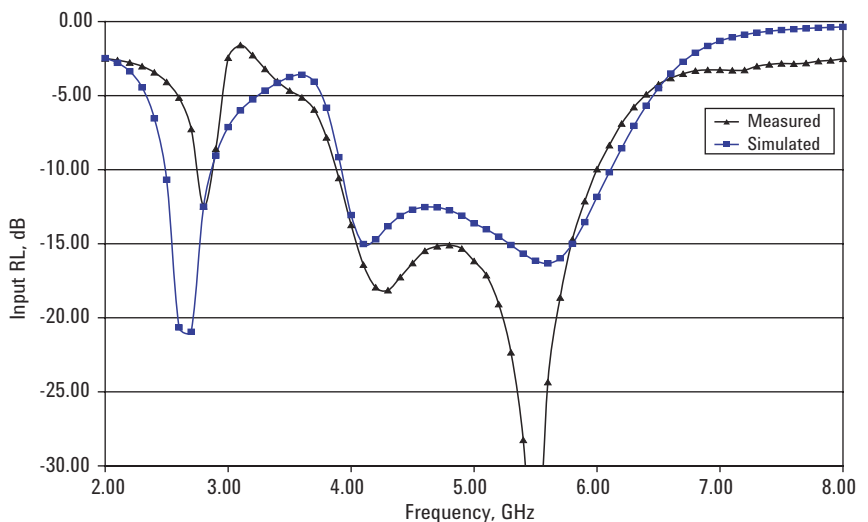


Figure 6. Measured and Simulated Input Return Loss vs. Frequency

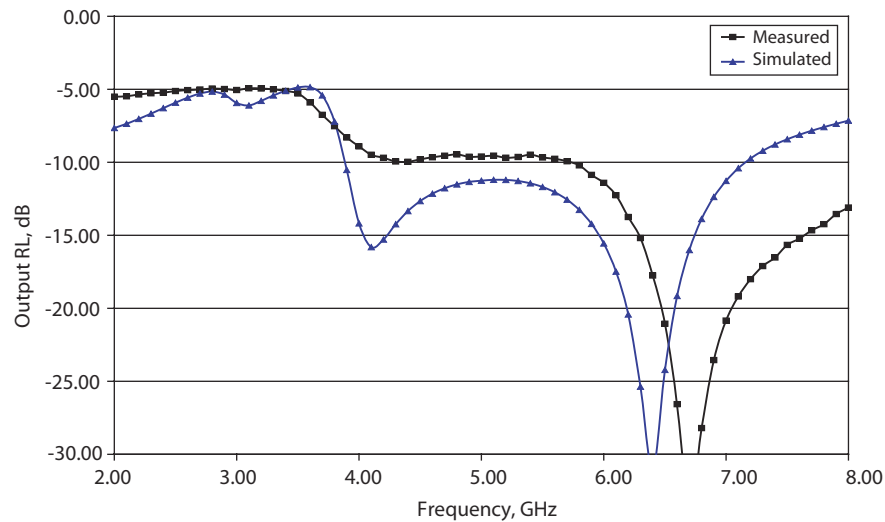


Figure 7. Measured and Simulated Output Return Loss vs. Frequency

Table 2. Summary of measured performance vs. supply voltage

	Supply, Vdd and Idd		
	3.3V, 30mA	3.0V, 23.3mA	2.7V, 15mA
Frequency, GHz	4.90		
Gain, dB	23.30	22.60	21.30
NF, dB	1.20	1.25	1.35
Frequency, GHz	5.50		
Gain, dB	22.32	21.90	21.00
NF, dB	1.30	1.37	1.45
Frequency, GHz	6.00		
Gain, dB	22.00	21.50	20.80
NF, dB	1.35	1.40	1.43

ADS Simulation Schematic

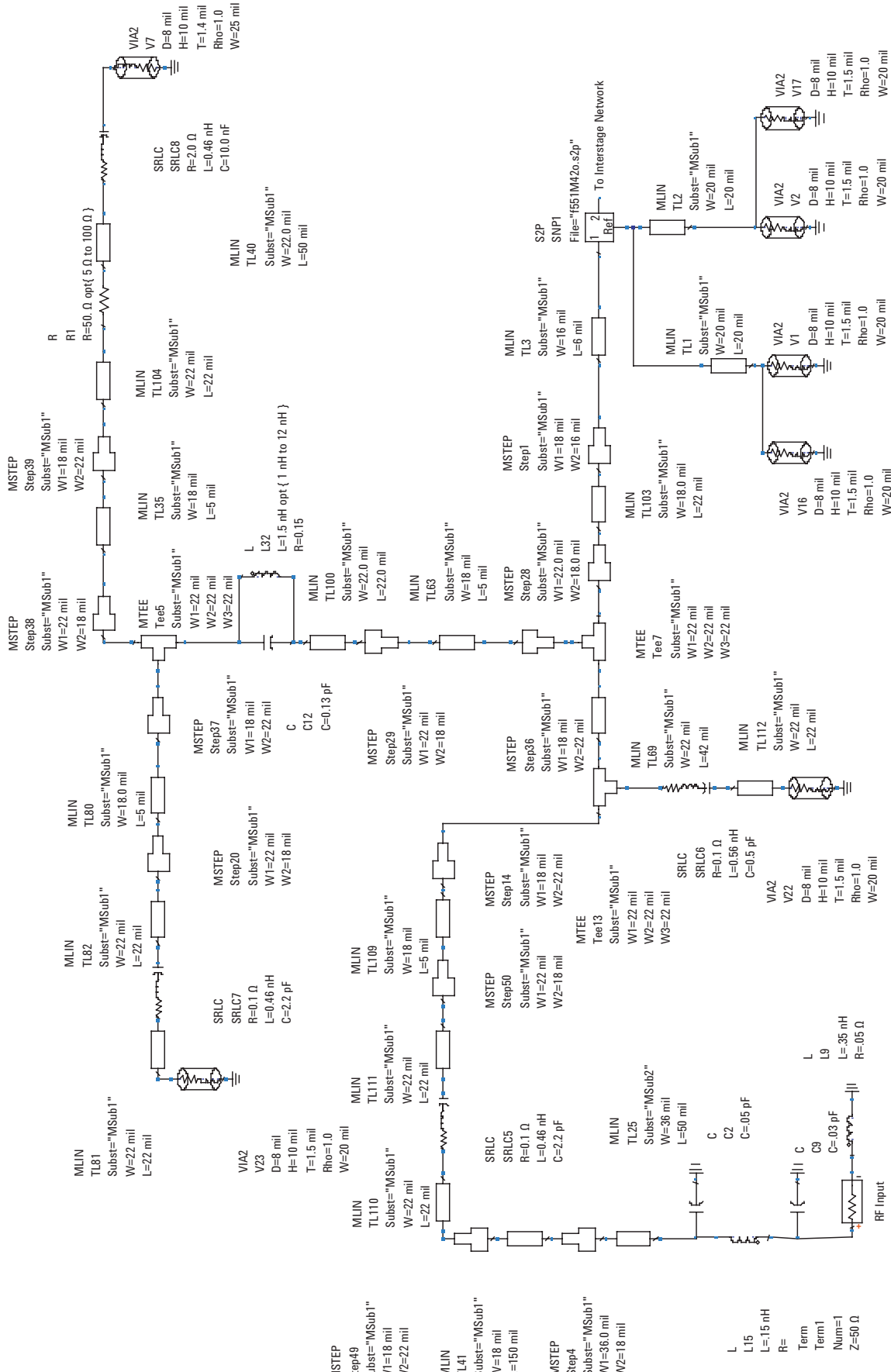


Figure 8. Input matching network. The empirically derived model for the EF Johnson end-launch SMA connector (p.n. 142-0701-801) is also shown.

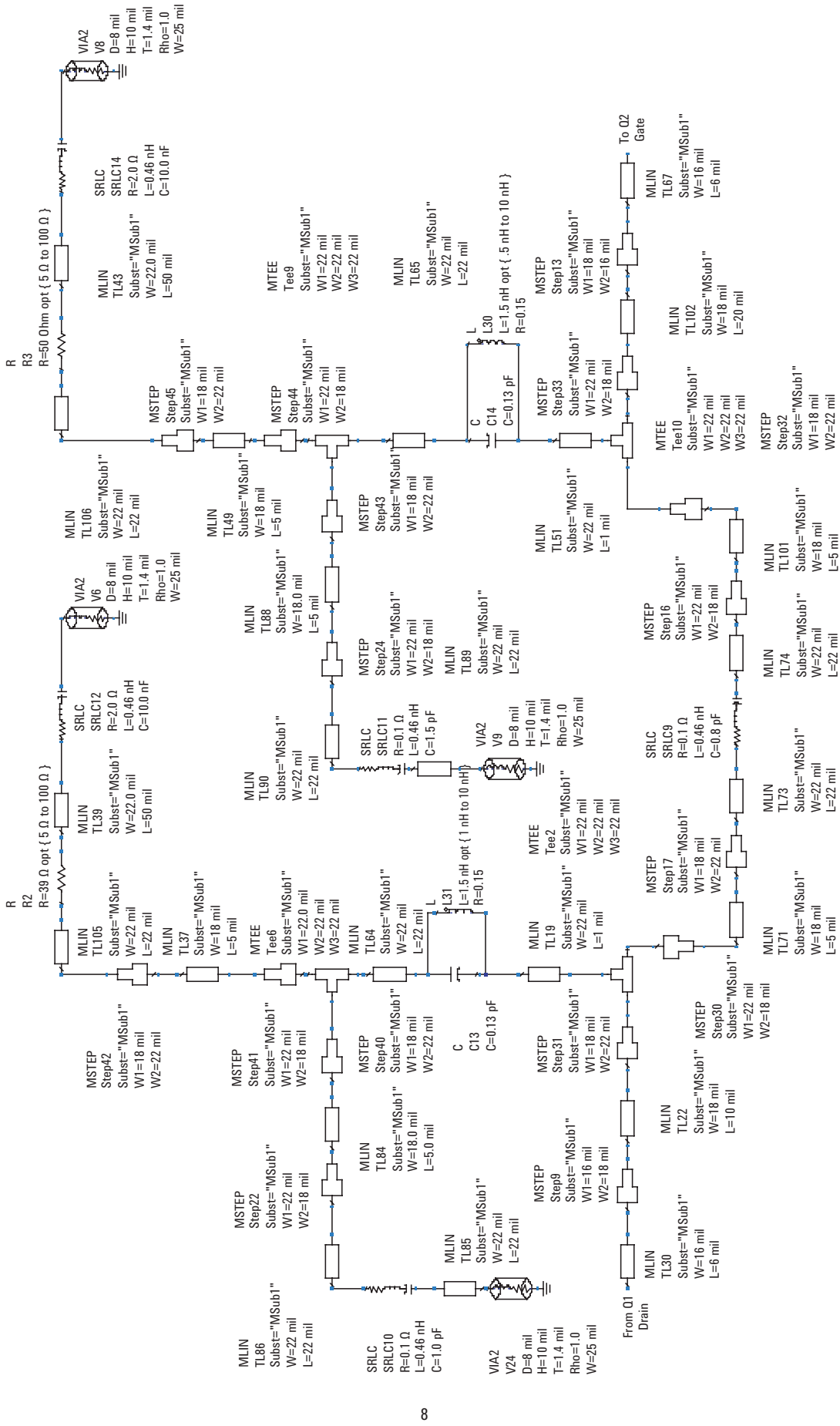


Figure 9. Interstage matching network

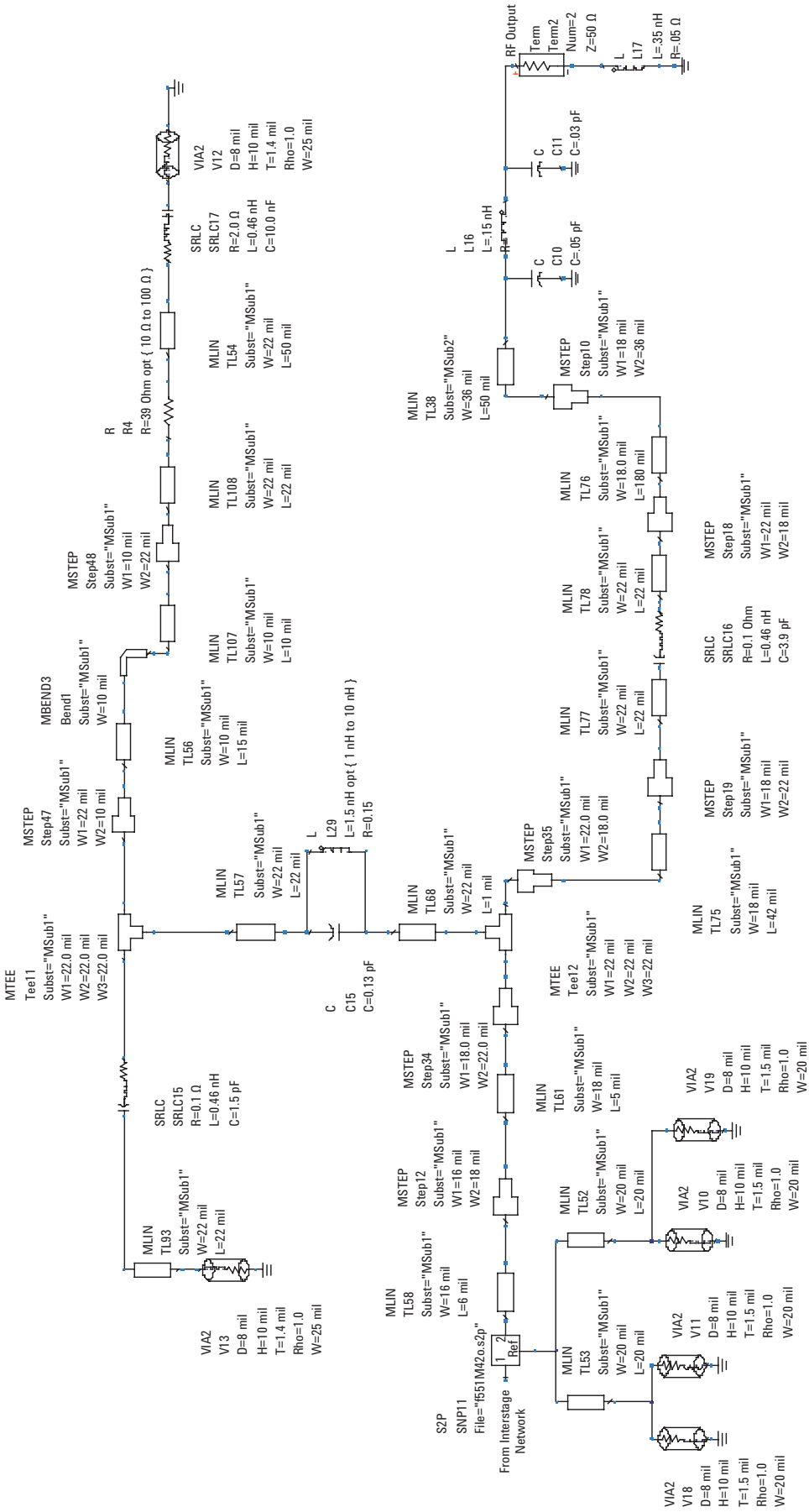


Figure 10. Output matching network. The empirically derived model for the EF Johnson end-launch SMA connector (p.n. 142-0701-801) is also shown.

OPTIM	MSub	MSub	S-PARAMETERS
Optim Optim1 OptimType=Gradient ErrorForm=L2 MaxIter=50 DesiredError=0.0 StatusLevel=4 FinalAnalysis="SP1" NormalizeGoals=no SetBestValues=yes Seed= SaveSolutions=no SaveGoals=yes SaveOptimVars=no UpdateDataset=yes SaveNominal=yes SaveAllIterations=no	UseAllOptVars=yes UseAllGoals=yes SaveCurrentEF=no MSUB MSub2 H=10 mil Er=4.6 Mur=1 Cond=1.0E+50 Hu=3.9e+034 mil T=36 mil TanD=.01 Rough=0 mil  StabFact StabFact1 StabFact1=stab_fact(\$)	H=10 mil Er=4.6 Mur=1 Cond=1.0E+50 Hu=3.9e+034 mil T=36 mil TanD=.01 Rough=0 mil  Mu Mu1 Mu1=mu(\$)	S_Param SP1 Start=2.0 GHz Stop=8.0 GHz Step=0.1 GHz
GOAL	GOAL	GOAL	OPTIONS
Goal OptimGoal1 Expr="dB(S(2,1))" SimInstanceName="SP1" Min=23 Max= Weight=100 RangeVar[1]="freq" RangeMin[1]=4.9e9 RangeMax[1]=6e9	Goal OptimGoal2 Expr="dB(S(1,1))" SimInstanceName="SP1" Min= Max=-13 Weight=50 RangeVar[1]="freq" RangeMin[1]=4.7e9 RangeMax[1]=6e9	Goal OptimGoal3 Expr="dB(S(2,2))" SimInstanceName="SP1" Min= Max=-13 Weight=50 RangeVar[1]="freq" RangeMin[1]=4.7e9 RangeMax[1]=6e9	Options Options1 Temp=16.85 Tnom=25 TopologyCheck=yes ForceS_Params=yes V_RelTol=1e-6 I_RelTol=1e-6 GiveAllWarnings=yes MaxWarnings=10
GOAL	GOAL	GOAL	
Goal OptimGoal5 Expr="dB(S(2,1))" SimInstanceName="SP1" Min= Max=15 Weight= RangeVar[1]="freq" RangeMin[1]=0.5E9 RangeMax[1]=3e9	Goal OptimGoal7 Expr="Mu1" SimInstanceName="SP1" Min=1 Max= Weight=200 RangeVar[1]="freq" RangeMin[1]=0.1e9 RangeMax[1]=18e9	Goal OptimGoal4 Expr="nf(2)" SimInstanceName="SP1" Min= Max=1.1 Weight= RangeVar[1]="freq" RangeMin[1]=4.8e9 RangeMax[1]=6e9	

Figure 11. Optimization simulation tool with target goals from schematic window

References:

- [1] Ward, A. Agilent ATF-54143 Low Noise Enhancement Mode Pseudomorphic HEMT in a Surface Mount Plastic Package, 2001 [Internet]. Available from: <http://literature.agilent.com/litweb/pdf/5988-9006EN.pdf>.

www.agilent.com/semiconductors

Product specifications and descriptions in this document subject to change without notice.

© Agilent Technologies, Inc. 2009
Printed in USA, May 5, 2009
5989-1609EN



Agilent Technologies

射 频 和 天 线 设 计 培 训 课 程 推 荐

易迪拓培训(www.edatop.com)由数名来自于研发第一线的资深工程师发起成立，致力并专注于微波、射频、天线设计研发人才的培养；我们于 2006 年整合合并微波 EDA 网(www.mweda.com)，现已发展成为国内最大的微波射频和天线设计人才培养基地，成功推出多套微波射频以及天线设计经典培训课程和 ADS、HFSS 等专业软件使用培训课程，广受客户好评；并先后与人民邮电出版社、电子工业出版社合作出版了多本专业图书，帮助数万名工程师提升了专业技术能力。客户遍布中兴通讯、研通高频、埃威航电、国人通信等多家国内知名公司，以及台湾工业技术研究院、永业科技、全一电子等多家台湾地区企业。

易迪拓培训课程列表：<http://www.edatop.com/peixun/rfe/129.html>



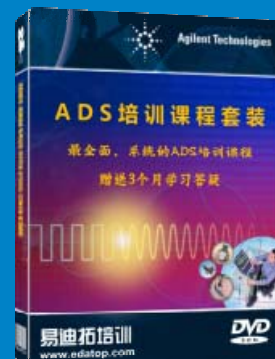
射频工程师养成培训课程套装

该套装精选了射频专业基础培训课程、射频仿真设计培训课程和射频电路测量培训课程三个类别共 30 门视频培训课程和 3 本图书教材；旨在引领学员全面学习一个射频工程师需要熟悉、理解和掌握的专业知识和研发设计能力。通过套装的学习，能够让学员完全达到和胜任一个合格的射频工程师的要求…

课程网址：<http://www.edatop.com/peixun/rfe/110.html>

ADS 学习培训课程套装

该套装是迄今国内最全面、最权威的 ADS 培训教程，共包含 10 门 ADS 学习培训课程。课程是由具有多年 ADS 使用经验的微波射频与通信系统设计领域资深专家讲解，并多结合设计实例，由浅入深、详细而又全面地讲解了 ADS 在微波射频电路设计、通信系统设计和电磁仿真设计方面的内容。能让您在最短的时间内学会使用 ADS，迅速提升个人技术能力，把 ADS 真正应用到实际研发工作中去，成为 ADS 设计专家…



课程网址：<http://www.edatop.com/peixun/ads/13.html>



HFSS 学习培训课程套装

该套课程套装包含了本站全部 HFSS 培训课程，是迄今国内最全面、最专业的 HFSS 培训教程套装，可以帮助您从零开始，全面深入学习 HFSS 的各项功能和在多个方面的工程应用。购买套装，更可超值赠送 3 个月免费学习答疑，随时解答您学习过程中遇到的棘手问题，让您的 HFSS 学习更加轻松顺畅…

课程网址：<http://www.edatop.com/peixun/hfss/11.html>

CST 学习培训课程套装

该培训套装由易迪拓培训联合微波 EDA 网共同推出，是最全面、系统、专业的 CST 微波工作室培训课程套装，所有课程都由经验丰富的专家授课，视频教学，可以帮助您从零开始，全面系统地学习 CST 微波工作的各项功能及其在微波射频、天线设计等领域的设计应用。且购买该套装，还可超值赠送 3 个月免费学习答疑…



课程网址: <http://www.edatop.com/peixun/cst/24.html>



HFSS 天线设计培训课程套装

套装包含 6 门视频课程和 1 本图书，课程从基础讲起，内容由浅入深，理论介绍和实际操作讲解相结合，全面系统的讲解了 HFSS 天线设计的全过程。是国内最全面、最专业的 HFSS 天线设计课程，可以帮助您快速学习掌握如何使用 HFSS 设计天线，让天线设计不再难…

课程网址: <http://www.edatop.com/peixun/hfss/122.html>

13.56MHz NFC/RFID 线圈天线设计培训课程套装

套装包含 4 门视频培训课程，培训将 13.56MHz 线圈天线设计原理和仿真设计实践相结合，全面系统地讲解了 13.56MHz 线圈天线的工作原理、设计方法、设计考量以及使用 HFSS 和 CST 仿真分析线圈天线的具体操作，同时还介绍了 13.56MHz 线圈天线匹配电路的设计和调试。通过该套课程的学习，可以帮助您快速学习掌握 13.56MHz 线圈天线及其匹配电路的原理、设计和调试…



详情浏览: <http://www.edatop.com/peixun/antenna/116.html>

我们的课程优势:

- ※ 成立于 2004 年，10 多年丰富的行业经验，
- ※ 一直致力并专注于微波射频和天线设计工程师的培养，更了解该行业对人才的要求
- ※ 经验丰富的一线资深工程师讲授，结合实际工程案例，直观、实用、易学

联系我们:

- ※ 易迪拓培训官网: <http://www.edatop.com>
- ※ 微波 EDA 网: <http://www.mweda.com>
- ※ 官方淘宝店: <http://shop36920890.taobao.com>